Proceedings of the XVII ECSMGE-2019
Geotechnical Engineering foundation of the future
ISBN 978-9935-9436-1-3

doi: 10.32075/17ECSMGE-2019-0134

XVII European Conference
ECSMGE 2019
Reykjavik
on Soil Mechanics
and Geotechnical Engineering

The response of framed buildings on raft foundations to tunnelling: a centrifuge and numerical modelling study

La réponse des bâtiments encadrés sur des fondations de radeaux au tunneling: une étude de centrifugation et de modélisation numérique

Jingmin Xu, Alec M. Marshall: *University of Nottingham, Nottingham, United Kingdom*
Andrea Franza: *Universidad Politécnica de Madrid, Madrid, Spain*
Daniela Boldini:*University of Bologna, Bologna, Italy*
Angelo Amorosi: *Sapienza University of Rome, Rome, Italy*
Matthew J. DeJong: *University of California, Berkeley, USA*

ABSTRACT: The expansion of cities often involves tunnel construction, which may result in detrimental effects on existing structures. This paper considers the interaction between tunnelling-induced ground deformations and framed buildings on raft foundations. The aim of the paper is to study the differences between scenarios where an equivalent plate and a real frame are used in the tunnel-building interaction problem. The paper includes experimental data obtained from geotechnical centrifuge tests and predictions of building response based on numerical analyses. The centrifuge experiments involved framed building models with walls extending in the direction of the tunnel axis. Digital image analysis was used to measure soil and building displacements during simulated tunnel volume loss. Results are compared to existing data from centrifuge tests that used an equivalent plate approach. Numerical simulations carried out with simplified and advanced Finite Element methods, performed respectively before (i.e class A predictions) and after (i.e. class C predictions) the centrifuge tests, are presented. Both methods effectively predict the soil and building deformation profiles determined experimentally. Finally, the potential for errors resulting from the equivalent plate approach are also discussed.

RÉSUMÉ: L'expansion des villes implique souvent la construction de tunnels, ce qui peut avoir des effets néfastes sur les structures existantes. Cet article examine l'interaction entre les déformations du sol induites par les tunnels et les bâtiments en ossature sur fondations en radier. Le but de cet article est d'étudier les différences entre des scénarios dans lesquels une plaque équivalente et une ossature réelle sont utilisées dans le problème de l'interaction tunnel-bâtiment. Cet article comprend des données expérimentales obtenues à partir d'essais géotechniques par centrifugation et des prévisions de la réponse du bâtiment basées sur des analyses numériques. Les expériences de centrifugation impliquent des modèles de construction construits avec des murs s'étendant dans la direction de l'axe du tunnel. L'analyse numérique des images a été utilisée pour mesurer les déplacements du sol et des bâtiments au cours de la simulation de la perte de volume de tunnel. Les résultats sont comparés aux données existantes issues d'essais en centrifugeuse utilisant une approche par plaque équivalente. Des simulations numériques effectuées à l'aide de méthodes simplifiées et avancées d'éléments finis, effectuées respectivement avant (prédictions de classe A) et après (prédictions de classe C), sont présentées. Les deux méthodes permettent de prédire de manière efficace les profils de déformation du sol et du bâtiment déterminés expérimentalement. Enfin, les possibilités d'erreur résultant de l'approche par plaque équivalente sont également discutées.

Keywords: Soil-structure interaction; Building response; Tunnels; Framed structure; Equivalent plate

1 INTRODUCTION

Tunnelling is common in urban areas because of the difficulty of finding available space in increasingly congested cities. Despite the use of advanced tunnel boring machines, tunnelling still causes ground movements which can affect nearby structures. Therefore, engineers need to predict the effects that tunnel constructions can have on buildings and infrastructure along the tunnel route.

Despite several studies indicating the importance of considering realistic framed building characteristics (Goh and Mair, 2014; Boldini et al., 2018), equivalent beam or plate models with cross-sectional properties calibrated using the equivalent stiffness of the real building (i.e. the equivalent solid approach) are still generally adopted (Potts and Addenbrooke, 1997; Franzius et al., 2006). This simplification, possibly reasonable in some cases, is characterised by numerous uncertainties not yet sufficiently investigated. Firstly, in estimating equivalent stiffness of a real building, studies have adopted the parallel axis theorem (Potts and Addenbrooke, 1997), taking the algebraic sum of individual bending stiffness of all floor slabs (Meyerhof 1953), and using a column stiffening factor approach (Meyerhof, 1953; Goh and Mair, 2014). Secondly, the equivalent beam/plate approach "averages" the distortions of each bay, without describing the local deformations of each structural element.

This study aims to [i] provide experimental evidence of tunnel-framed building interaction, for which there is a lack of available experimental data, [ii] estimate the effects of implementing the equivalent solid approach within tunnel-structure interaction (TSI) analyses by comparison with centrifuge results, and [iii] highlight the capability of simplified and advanced numerical approaches to provide reliable class A and C predictions (Lambe, 1973) of the problem. The paper presents new centrifuge data of tunnelling effects on a 2-storey framed building and compares the results with those of centrifuge tests in which an equivalent solid approach was adopted (Farrell, 2010). Numerical analyses of the tests are also discussed and used to provide further insights into the soil-structure interaction problem.

2 CENTRIFUGE STUDY

2.1 Experimental package, building model, and procedure

The 4 m diameter geotechnical centrifuge at the University of Nottingham Centre for Geomechanics was used to perform the tests. A plane-strain package including a strongbox and flexible membrane model tunnel was used alongside a fine dry silica sand known as, Leighton Buzzard Fraction E.

In order to compare results against Farrell's data (2010), which employed 1.6, 5, 10, and 20 mm thick plates (labelled STR1 to STR4, respectively), the same prototype scenario was considered, in which a tunnel with diameter D_t = 6.1 m and cover depth C = 8.0 m (C/D = 1.3) was centrally constructed beneath a building with a transverse width B = 30 m under plane-strain conditions. The tests presented here were performed at 68 g, instead of 75 g used by Farrell, due to the difference in model tunnel diameters (D_t = 82 mm for Farrell). A 2-storey framed aluminium building model was machined for this study. The model was 258 mm long in the tunnel longitudinal direction, leaving a 1mm gap at the front/back walls of the centrifuge box. The thicknesses (t) of the raft foundation, beams/slabs, and columns/walls of the building model are all 3.2 mm. Each storey includes 6 bays, the width (b_{bay}) and height (h_{storey}) of which are 76.2 mm and 38.1 mm, respectively, giving a total height of 79.4 mm. Figure 1 provides dimensions of the framed structure at model scale. The framed building model was machined by welding two aluminium alloy plates and 12 angle sections. A rigid connection was achieved by welding 60% of the

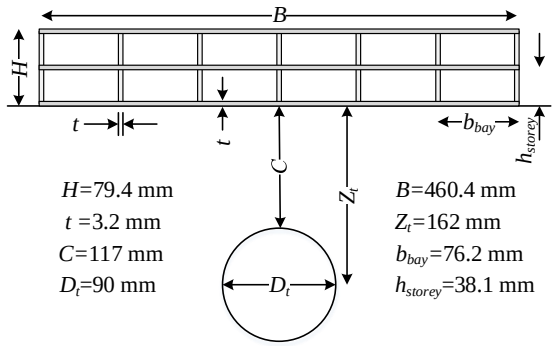

Figure 1. Experiment layout (model scale).

length along the longitudinal direction (see top of model in Figure 2). To replicate a rough soil-foundation interface, a thin layer of sand was bonded beneath the structure. White dots were painted on the front face of the foundation, beams, and columns/walls to enable digital image analysis (GeoPIV; White et al., 2003) of soil and structure displacements.

The test procedure consisted of: 1) after air pluviation of soil to a relative density I_d = 90%, the building model was placed on the surface at 1 g (not required for greenfield test); 2) the package was mounted on the centrifuge and spun to 68 g; 3) the tunnel volume loss $V_{l,t}$ was simulated in 0.1% increments up to 3%, 0.2% increments up to 5%, and 0.5% increments up to 10% (images were taken at each increment); 4) the centrifuge was spun down.

2.2 Experimental results

2.2.1 Evaluation of frame stiffness

To facilitate comparison between results, the equivalent bending stiffness of the structural models adopted in the centrifuge tests are given in Table 1 at prototype scale. Bending stiffness is quantified in terms of [i] equivalent cross-sectional flexural rigidity EI_{str} and EI_{frame} for Farrell's plates and the tested frame, respectively, [ii] the thickness of an equivalent plate, t_{equiv}, and [iii] $\log_{10}(EI)$, which is useful considering that TSI varies with the log scale of relative soil-structure stiffness (Potts and Addenbrooke, 1997; Franzius et al., 2006). A three-point bending test was conducted to obtain the experimental (EXP) values of EI_{frame} using Euler-beam theory, whereas the formulas from Goh and Mair (2014) were also used to obtain the analytical (AN) values. In both cases a Young's modulus E = 70 GPa was assumed, and the entire structure was assumed to be in sagging. Table 1 shows that the analytical and experimental values of EI_{frame} are slightly larger than EI_{str} for STR3. However, the experimental value indicates that the real stiffness of the frame is close to the values of the STR3 plate, thus hereafter only STR3 is considered for comparison of results.

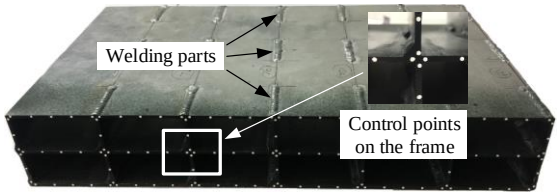

Figure 2. Framed building model.

Table 1. Summary of building stiffness.(prototype)

	EI_{str}/m, EI_{frame}/ m (GNm)	t_{equiv} (m)	$\mathrm{Log}_{10}(EI/\mathrm{m})$ (Nm)
STR2	0.3	0.38	8.5
STR3	2.5	0.75	9.4
STR4	20	1.5	10.3
FR.AN.	4.8	0.93	9.7
FR.EXP.	3.2	0.82	9.5

2.2.2 Comparison of results

The settlements and horizontal displacements of the foundation, first-storey (middle plate) and second storey (top plate) of the frame at a tunnel volume loss $V_{l,t}$ = 2% are presented in Figure 3(a) and (c), all at prototype scale. Data for the 10 mm thick plate (STR3) obtained by Farrell (2010) are also presented in Figure 3(b) and (d). The foundation of the frame is noted to have settled slightly more than the soil beneath it at the edges of the model structure. This "error" is probably caused by the fact that the face side of the frame is not perfectly in contact with the inner surface of the Perspex window.

The same issue was also found in previous experiments (Farrell, 2010, Ritter et al., 2017).

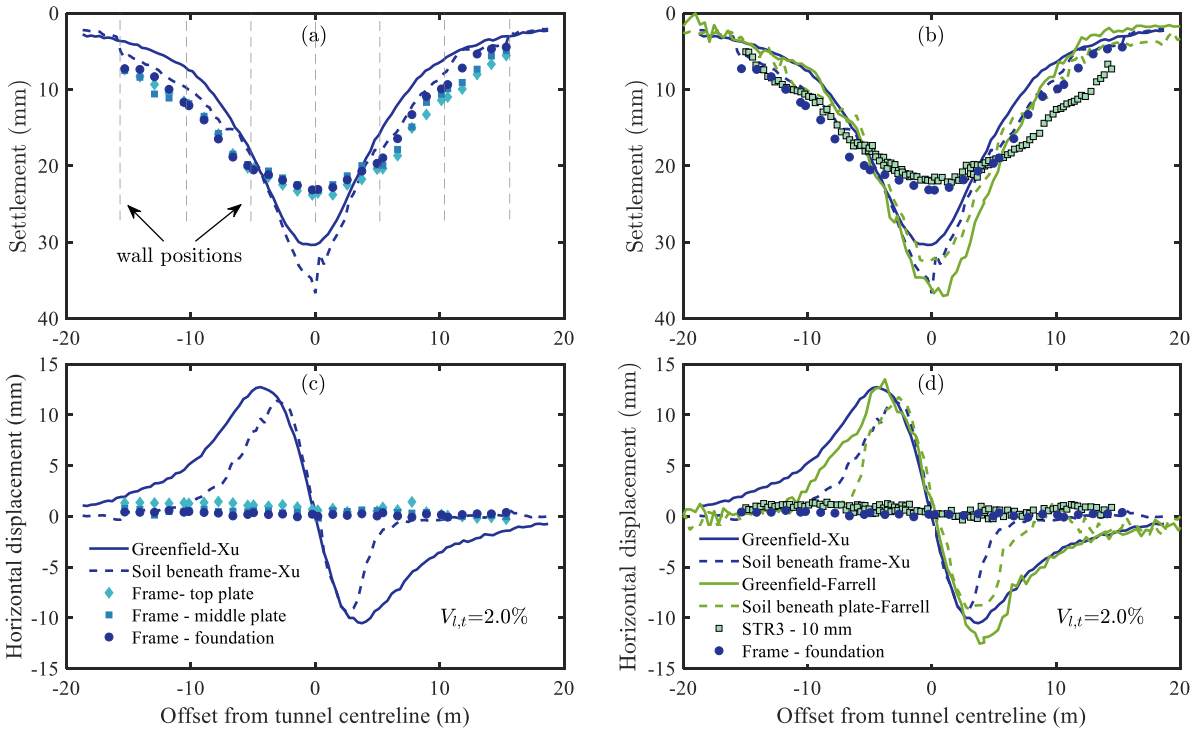

Figure 3 Experimental result and comparison with centrifuge data obtained by Farrell (2010).

It should also be noted that, due to the differences in the experimental packages (for example, tunnel longitudinal length) and the size of the centrifuge, the shape and magnitude of the greenfield settlement trough in this study are slightly different from Farrell's data. This can be seen in Figure 3 (b), where Farrell's settlements above the tunnel centreline are larger, thus resulting in a narrower profile. Figure 3 (b) also shows that the soil beneath the frame settled more than in greenfield conditions, which was not the case for the plate tests by Farrell. The reasons and consequences of these differences are under investigation; however for now their effects on the TSI mechanism are considered secondary.

Figure 3 (a) indicates that a gap formed at the soil-structure interface (the difference between the dashed line and the foundation markers). This agrees with the STR3 results presented in Figure 3 (b). However, the settlement curves of the frame are characterized by distinct changes in slope at the wall positions, which is different to the smooth curves of the equivalent plate data from Farrell (2010). This is due to the localised tunnelling-induced axial forces and bending moments applied by the wall to the raft. The centrifuge tests show that the columns not only increase the bending stiffness of the building (according to Goh and Mair, 2014), but also vary the slope of the foundation settlement curve in the framed building. In the equivalent plate approach this latter effect cannot be captured, thus possibly underestimating the building deformations. Furthermore, the settlement profile of the frame foundation consists of both sagging and hogging regions, while the equivalent plates from Farrell mostly display a sagging deformation mode. Horizontal displacements in Figures 3 (c) and (d) show that both the frame and the plates responded rigidly to tunnelling in the horizontal direction. The

friction generated by the foundation roughness and building self-weight restricted the soil surface horizontally, especially close to the structure edges (Ritter et al., 2017). On the other hand, significant slippage at the soil-structure interface was measured at the centre of the frame because of vertical load redistribution from the structure centre towards the edges due to the building stiffness (also associated with the gap formation (Franza and DeJong, 2018).

3 SIMPLIFIED NUMERICAL STUDY (CLASS A PREDICTIONS)

3.1 FEM Model

Class A predictions of the TSI problem were obtained via the program ASRE (Franza and DeJong, 2018). This simplified Finite Element Method (FEM) model implements a two-stage analysis method. It considers the structure as a plane frame (consisting of Euler-Bernoulli beams) resting on an elastic homogeneous half-space continuum subjected to forces equivalent to the greenfield tunnelling-induced ground movements. The soil-foundation interface consists of perfectly plastic sliders that account for slippage and gap formation by limiting horizontal and vertical tensile forces. The superstructure (i.e. all structural elements above foundation level) stiffness and loading were modelled by condensing the superstructure contribution to the nodes of the foundation elements. Because of the sliders, the self-weight loads need to be applied prior to tunnelling to capture the possible gap formation and slippage at the soil-structure interface. In the simplified FE model, inputs consist of the problem geometry, elasticity parameters of the structure and the soil, greenfield soil movements, and structure loadings. The geometrical parameters in the plane transverse to the tunnel axis were set equal to the centrifuge scenario at prototype scale. The superstructure and foundation lengths in the tunnel longitudinal direction (also defining the area of soil beneath the raft) were set equal to 10 m. The offset between the raft axis and the ground level was neglected. A finite element size of 1.05m was adopted in the transversal direction to the tunnel axis. For the soil continuum, a Young's modulus of $E_s = 45$ MPa and a Poisson's ratio of $\nu = 0.3$ were assumed, while for the structure $E = 70$ GPa. The E_s value was selected to account for the average stiffness of the soil above the tunnel following the procedure detailed by Farrell (2010). The friction coefficient between the soil and foundation was set to $\mu = \tan(32°)$, which corresponds to the soil critical state friction angle. Greenfield vertical and horizontal movements up to a maximum $V_{l,t} = 5\%$ were obtained by interpolating the greenfield movements measured by Farrell (2010) with empirical curves; for further details on curve-fitting refer to Franza and DeJong (2018). Finally, self-weight loads per unit length of the beam elements that were used to model walls, slabs and the raft were computed from the beam cross-sectional geometry by specifying a specific weight of 27 kN/m^3 for the structure.

3.2 Numerical results

Centrifuge results are compared against the simplified numerical model (ASRE) Class A predictions in Figure 4. Firstly, the tunnelling-induced settlements shown in Figure 4 (a) illustrate that the foundation settlement profiles from ASRE and the centrifuge results are similar in shape. Thus, they are associated with comparable levels of deflection ratios, which are important for risk assessments. Horizontal movements in Figure 4(b) show that the ASRE solution predicted minimal horizontal differential displacements along the foundation, in agreement with the centrifuge measurements.

The ASRE solution was able to predict both the gap formation as well as the slippage at the soil-foundation interface (gap and slippage are given by the distance between dashed lines and markers in Figures 4 (a) and (b), respectively). This indicates that ASRE is able to describe the

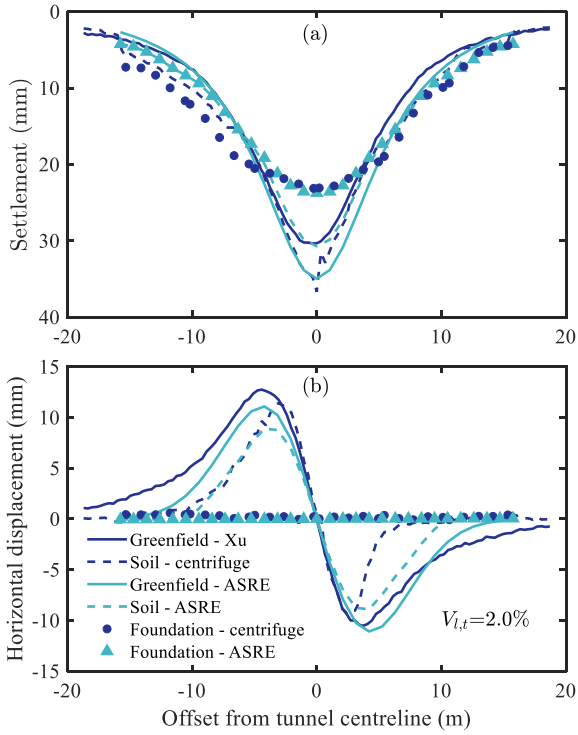

Figure 4 Experimental results and Class A predictions from the simplified numerical model.

tunnelling-induced redistribution of the self-weight load beneath the foundation.

These results provide evidence of the reliability of the ASRE solution for framed configurations. Notably, the minimal computational cost and small number of input parameters enabled the simplified numerical model analyses to be performed quickly prior to centrifuge testing. This preliminary simulation was used to optimise the experimental testing plan, which can be a challenging task in centrifuge modelling. Future work will evaluate the effect of varying the greenfield centrifuge inputs.

4 ADVANCED NUMERICAL STUDY (CLASS C PREDICTIONS)

4.1 FEM Model

A 3D numerical model was set up using the commercial Finite Element code Abaqus (version 6.14), the soil domain corresponding to the centrifuge box dimensions. Boundary conditions consisted of constrained horizontal displacements perpendicular to the lateral faces and null displacement components at the base of the model.

Soil response was modelled adopting the SANISAND bounding surface plasticity model of Dafalias and Manzari (2004). The constitutive law was found to realistically reproduce the behaviour of sands under different strain levels adopting a unique set of constitutive parameters. The model parameter values in Table 2 were selected based on a set of preliminary numerical analyses aimed at reproducing Farrell's (2010) centrifuge results. For the frame, an isotropic linear elastic law was considered, with the same parameters considered in the numerical study of section 3. 20-node quadratic brick elements with reduced integration were selected for the soil and the frame. The contact between the soil and the foundation was simulated by enforcing a no-penetration/sliding-friction contact interaction, with coefficient of friction equal to that of the soil at critical state (i.e. 32°), thus using contact mechanics laws rather than interface elements.

Table 2 Material constants of the SANISAND model for the Leighton Buzzard Fraction E

Elasticity	$G_0 = 400$; $\nu = 0.05$
Critical state	M_c=1.287; $c = 0.780$; $\lambda_c = 0.00178$; $e_0 = 0.8191$; $\xi = 2.4352$
Yield surface	$m = 0.01$
Plastic modulus	$h_0 = 4.05$; $c_h = 1.1$; $n^b = 2.8$
Dilatancy	$A_0 = 0.55$; $n^d = 2.564$
Fabric-dilatancy tensor	$z_{max} = 0$; $c_z = 0$

The analyses comprised the following stages: 1) gravity activation in the soil domain, assuming a coefficient of earth pressure at rest K_0=0.5; 2) activation of the frame elements and contact interaction (only in the TSI analysis); 3)

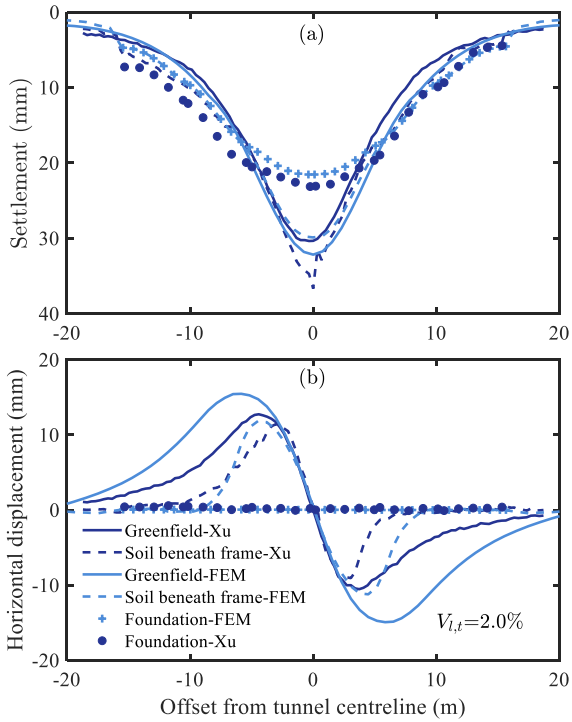

Figure 5 Experimental results and Class C predictions from the advanced numerical model

deactivation of soil elements inside the tunnel and application of incremental displacements at the boundary nodes. These displacements were set to obtain a homothetic contraction of the tunnel cross-section with a vertical translation such that the lower point of the tunnel remains in its initial position (Boldini et al., 2018).

4.2 Numerical results

The distribution of vertical and horizontal displacements at the ground surface obtained at the end of the analyses are shown in Figure 5a and 5b. For the TSI analysis both the soil and the frame displacements are plotted.

In general, displacements are well predicted by the FE simulation. The gap occurrence in the vertical direction as well as the horizontal slippage at the soil-structure interface are captured in the TSI analysis.

In contrast to the ASRE predictions, the maximum settlement of the frame is slightly underestimated while the magnitude of vertical displacements in the right portion of the structure, where a prevailing hogging pattern is observed, match the centrifuge results well. In the left portion of the frame the observed settlements are larger, given the non-symmetry of the profile, and the previous good agreement is partially lost.

The agreement between numerical results and measurements is slightly less good for the horizontal displacements experienced by the soil, especially under greenfield conditions. In the TSI analysis the frame is found not to suffer any horizontal strains, as observed in the centrifuge test. The displacement profile for the soil beneath the frame fits the centrifuge results well under the left portion of the structure, while this does not hold along the right side. However, as the experimental data are not completely symmetric with respect to the tunnel axis, the predicted trends can be considered satisfactory.

Vertical and horizontal displacements computed at the first and second floor of the frame were found to be very similar to those of the foundation. As such, to enhance clarity, they are not shown in Figure 5.

Numerical analyses, which employed advanced constitutive laws for the soil and for the soil-structure interface, were demonstrated to accurately predict soil and frame displacements. Once calibrated and validated against centrifuge data, the FE model could be employed to simulate more realistic soil-structure interaction problems or to analyse case-histories characterised by more complex geometries and geotechnical conditions.

5 CONCLUSIONS

This paper investigated the response of a framed building on a raft foundation to tunnel construction, both experimentally and numerically. The following conclusions can be drawn. Although gap formation and slippage were observed at the soil-structure interface for

both the frame and Farrell's equivalent plate test (STR3), the frame settlement curves were characterized by distinct changes in slope at the column/wall locations, which differ from the smooth curves of the equivalent plate data.

The simplified numerical model ASRE, which was used for the design of the experimental testing plan, was able to provide good Class A predictions of the tunnelling-induced foundation displacement distributions; this confirmed the reliability of this solution for preliminary assessments of the effect of tunnelling on an existing building above a proposed tunnel route.

Predictions obtained by the advanced FE approach also proved to effectively reproduce the centrifuge experimental results, providing some validation that this approach can be used for the investigation of more complex and realistic soil-frame interaction problems.

6 ACKNOWLEDGEMENTS

This project has received funding from the European Union's Horizon 2020 research and innovation programme under the Marie Sklodowska-Curie grant agreement No 793715.

7 REFERENCES

Boldini, D., Losacco, N., Bertolin, S., Amorosi, A. 2018. Finite element modelling of tunnelling-induced displacements on framed structures, *Tunnelling and Underground Space Technology* **80**, 222–231.

Dafalias, Y.F., Manzari, M.T. 2004. Simple plasticity sand model accounting for fabric change effects, *Journal of Engineering Mechanics* **130**, 622–634.

Farrell, R. 2010. *Tunnelling in sands and the response of buildings*, Ph.D. thesis, University of Cambridge, U.K.

Farrell, R., Mair, R., Sciotti, A., Pigorini, A. 2014. Building response to tunnelling, *Soils and Foundations* **54**, 269–279.

Franza, A., Acikgoz, S., DeJong, M.J. 2018. Linear models for the evaluation of the response of beams and frames to tunnelling. *Proceedings of the 9th European Conference on Numerical Methods in Geotechnical engineering* (Eds: Cardoso A.S. et al.), 1275–1283. Porto, Portugal: CRC Press/Balkema, Leiden, The Netherlands.

Franza, A., DeJong, M.J. 2019. Elastoplastic solutions to predict tunneling-induced load redistribution and deformation of surface structures, *Journal of Geotechnical and Geoenvironmental Engineering* **145**, 04019007.

Franzius, J.N., Potts, D.M., Burland, J.B. 2006. The response of surface structures to tunnel construction, *Proceedings of the ICE - Geotechnical Engineering* **159**, 3–17.

Goh, K.H., Mair, R.J. 2014. Response of framed buildings to excavation-induced movements, *Soils and Foundations* **54**, 250–268.

Lambe, T.W. 1973. Prediction in soil engineering, *Géotechnique* **23**, 149–202.

Meyerhof, G.G. 1953. Some recent foundation research and its application to design, *The Structural Engineer* **31**, 151–167.

Potts, D.M., Addenbrooke, T.I. 1997. A structure's influence on tunnelling-induced ground movements, *Proceedings of the Institution of Civil Engineers - Geotechnical Engineering* **125**, 109–125.

Ritter, S., Giardina, G., DeJong, M.J., Mair, R.J. 2017. Influence of building characteristics on tunnelling-induced ground movements, *Géotechnique* **67**, 1–12.

White, D., Take, W., Bolton, M. 2003. Soil deformation measurement using particle image velocimetry (PIV) and photogrammetry, *Géotechnique* **53**, 619–631.